Results in Physics 7 (2017) 3459–3464

Contents lists available at ScienceDirect

Results in Physics

journal homepage: www.journals.elsevier.com/results-in-physics

Enhancing the corrosion resistance of the 2205 duplex stainless steel bipolar plates in PEMFCs environment by surface enriched molybdenum

Lv Jinlong [a,*], Wang Zhuqing [b], Liang Tongxiang [c], Suzuki Ken [a], Miura Hideo [a]

[a] Fracture and Reliability Research Institute, School of Engineering, Tohoku University, Sendai 9808579, Japan
[b] Research Institute for Engineering and Technology of Tohoku Gakuin University, Sendai 985-8537, Japan
[c] School of Materials Science and Engineering, Jiangxi University of Science and Technology, Ganzhou 341000, Jiangxi, China

ARTICLE INFO

Article history:
Received 25 March 2017
Received in revised form 23 August 2017
Accepted 6 September 2017
Available online 12 September 2017

Keywords:
Surfaces
Structural materials
Microstructure
X-ray diffraction

ABSTRACT

Surface molybdenum enrichment on 2205 duplex stainless steel was obtained by the ball milling technique. The electrochemical results showed molybdenum enrichment on the surface of 2205 duplex stainless steel improved its corrosion resistance in a typical proton exchange membrane fuel cell environment. This was mainly attributed to higher molybdenum content in the passive film formed on 2205 duplex stainless steel after ball milling. The decreased donor and acceptor concentrations improved significantly the corrosion resistance of surface molybdenum-enriched 2205 duplex stainless steel bipolar plates in the simulated cathodic proton exchange membrane fuel cells environment. In addition, the interfacial contact resistance of the 2205 duplex stainless steel bipolar plates slightly decreased due to surface molybdenum enrichment.

Introduction

Proton exchange membrane fuel cell (PEMFCs) is a device that directly and efficiently converts chemical energy into electricity. Thus it is considered as a clean energy device beyond petroleum [1]. Non-porous graphite is regarded as excellent bipolar plates due to its high conductivity and excellent corrosion resistance. However, its main weakness is high cost, poor machining property and brittleness for portable application [2]. The stainless steels are also widely accepted as a promising bipolar plates materials [3]. However, its corrosion is still a serious problem in the acidic environment of PEMFC operation. In addition, the corrosion products tend to contaminate the catalysts and reduce the overall efficiency of the cell [4]. Laser surface alloying of 304 stainless steel with Mo could be an appropriate technique to enhance the resistance to pitting and erosion–corrosion in NaCl solution [5]. The formation of molybdenum insoluble oxides enhanced the corrosion performance of AISI 304 and 316 stainless steels in H_2SO_4 solution [6]. The enrichment of Cr and Mo in the oxide layer had improved the corrosion resistance of the AISI 304 and AISI 316 stainless steels [7,8]. Mo oxides decreased active surface sites of ferritic stainless steels in acid solution [9]. The potentiodynamic and potentiostatic tests in simulated PEMFCs operating conditions and interfacial contact resistance (ICR) measurement implied that the molybdenum nitride modified 304 stainless steel improved the corrosion resistance and ICR [10]. The study showed that the 316L stainless steel was in the passive state in simulating the cathode PEMFCs environment, moreover, the passive current density decreased and the passive potential region enlarged with increasing Mo content [11]. The compactness and corrosion resistance of the passive film formed on 316L stainless steel enhanced with the increasing of Mo content. Moreover, Mo decreased the donor and acceptor densities in the inner and outer layers of the passive films and increased the Cr_2O_3 content in the passive films. Compared with the uncoated 316L stainless steel, all the Ti-Mo-N film coated ones showed enhanced corrosion resistance in simulating the cathode PEMFCs environment [12]. However, when Mo content in the Ti-Mo-N films increased, the corrosion resistance of the Ti-Mo-N film gradually degraded. In addition, the investigation showed that molybdate firstly formed in the passive film and then later partially dissolved into a solution [13].

Despite some studies focused on the effect of the Mo on the passivity of austenitic stainless steel, the studies on the effect of surface molybdenum enrichment on the corrosion behaviors of the 2205 duplex stainless steel in simulating the cathode PEMFCs environment was still scarce. Therefore, the objective of this work is to investigate the effect of surface molybdenum enrichment by ball milling on the corrosion behavior of 2205 duplex stainless steel in the simulated PEMFCs cathodic environment by electrochemical

* Corresponding author.
E-mail address: ljltsinghua@126.com (L. Jinlong).

http://dx.doi.org/10.1016/j.rinp.2017.09.001
2211-3797/

experiment and X-ray photoelectron spectroscopy analysis. In addition, the effect of surface molybdenum enrichment on ICR was also evaluated.

Experimental

Material preparation and characterization

The chemical composition of used 2205 duplex stainless steel in weight percent was 0.05 C, 1.05 Mn, 0.022 P, 0.0008 S, 0.75 Si, 21.85 Cr, 5.36 Ni, 3.18 Mo, 0.18 Cu, 0.13 V, 0.054 W, 0.015 Ti, 0.155 N and Fe balance. The as-received samples were annealed at 1100 °C for 1 h and water-quenched for solution treatment. The 2205 duplex stainless steel plate was cut to square with a dimension of 10 mm × 10 mm × 1 mm for test. The sample and nano Mo powder mixtures were loaded into a vacuum ball milling tank with stainless steel balls. The ball to powder weight ratio was 10:1. The ball milling process was performed at a rotational speed of 300 rpm for 300 h at room temperature. The milling process was periodically interrupted for half an hour every 2 h to avoid excessive heating of the vials. The X-ray diffraction (XRD) measurement was carried out by a Rigaku Ultima IV diffractometer using Cu K_α (0.154056 nm) by radiation at 40 kV and 40 mA. Scanning Electron Microscope (SEM JSM5800) was used for morphology observation.

Electrochemical test

CHI660E electrochemical workstation (Chenhua instrument Co. Shanghai, China) was used for electrochemical measurements. The counter electrode is a large thin platinum foil and the saturated calomel electrode (SCE) is the reference electrode. The potential described in this study is relative to the SCE. The electrochemical tests were conducted in 0.5 M H_2SO_4 solution with 2 ppm HF solution at 70 °C. The applied potentiostatic polarizations were carried out at 0.6 V_{SCE} in air-purged solution for simulating the cathode PEMFCs environment. The electrochemical impedance spectroscopy (EIS) measurements in cathode PEMFCs environment also were conducted at 0.6 V_{SCE}. The peak to peak amplitude of the sinusoidal perturbation signals of 5 mV was used during the EIS measurements. The frequency ranged from 100 kHz to 10 mHz.

X-ray photoelectron spectroscopy (XPS) measurement

The surface compositions of two 2205 duplex stainless steels were analyzed by X-ray photoelectron spectroscopy (XPS, PHI Quantera SXM) with monochromatized Al Ka source. The binding energy and relative intensity were analyzed to obtain further information about the chemical states of surface passive films. The C 1s peak from adventitious carbon at 284.8 eV was used as a reference to correct the charging shifts. XPSPeak4.1 software was used to fit obtained XPS experiment data.

ICR test

The ICR was obtained by measuring the voltage drop across the surface contacts at room temperature. The ICR between the sample and carbon paper was measured. Two pieces of carbon papers were sandwiched between the stainless steel and two copper plates. An outside force was applied on the two insulators above and below copper plates, respectively. The needed compaction force was applied by weight which was provided by a sanki hydraulic press. A milliohm meter (ZY9858) with a resolution of 0.1 μΩ was used for measurement of total resistance under different compaction forces. The compaction forces changed from 50 to 500 N cm^{-2}.

Results and discussion

The surface morphology of solid solution 2205 duplex stainless steel is shown in Fig. 1a. The microstructure of the solution annealed sample shows bulgy ferritic phase and concave austenitic phase. The surface is undulating for molybdenum-enriched 2205 duplex stainless steel in Fig. 1b. Liu et al. [14] reported significant grain refinement and severe plastic deformation in the top layer for 316L stainless steel as a result of ultrasonic shot peening. XRD was used to study the phase transformations due to ball milling and surface molybdenum. The ferritic and austenitic phases are detected in solid solution 2205 duplex stainless steels by XRD owing to their different crystal structure in Fig. 1c. After ball milling and surface molybdenum enrichment, the intensities of the diffraction peaks of ferritic and austenitic phases significantly change. Moreover, some strain induce α'-martensitic phases are observed after ball milling and surface molybdenum enrichment due to several plastic deformation. It is worthwhile to note that the ferritic phase has a preferred orientation (1 1 0) in solution annealed 2205 duplex stainless steel, while ferrite and α'-martensite expand along a preferred orientation (2 0 0) in surface molybdenum-enriched 2205 duplex stainless steel in Fig. 1b. Moreover, the austenitic phase has a preferred orientation (1 1 1) in solution annealed 2205 duplex stainless steel, while austenitic phase expands along a preferred orientation (2 2 0) in surface molybdenum-enriched 2205 duplex stainless steel. No intermetallic compounds are observed in surface molybdenum-enriched 2205 duplex stainless steel.

The result of Energy Dispersive Spectrometer shows that the chromium and molybdenum enrichment in ferritic phase in Fig. 2a, while nitrogen and nickel enrichment in austenitic phase for solution annealed 2205 duplex stainless steel in Fig. 2b. The result of Energy Dispersive Spectrometer also shows that the molybdenum enriches significantly on ball milled 2205 duplex stainless steel in Fig. 1c.

Fig. 3a shows anodic polarization curves for solid solution and surface molybdenum-enriched 2205 duplex stainless steels in cathode PEMFCs environment. The results of potentiodynamic tests show that solid solution and surface molybdenum-enriched 2205 duplex stainless steels have similar corrosion potential and breakdown potential in cathode PEMFCs environment. However, surface molybdenum-enriched 2205 duplex stainless steel has lower passivated current than solid solution one in cathode PEMFCs environment. This indicates that enriched molybdenum on the surface by ball milling inhibits the dissolution of the passive film on 2205 duplex stainless steel bipolar plates in cathode PEMFCs environment. Therefore, it can be concluded that the surface molybdenum-enriched 2205 duplex stainless steel is suitable as the bipolar plates in cathode PEMFCs environment.

In order to further evaluate the corrosion resistance of solid solution and surface molybdenum-enriched 2205 duplex stainless steels in the cathode environment for a long-term operation, the potentiostatic test was carried out. The current density as a function of time at 0.6 V_{SCE} is obtained. Fig. 3b show transient currents curves of solid solution and surface molybdenum-enriched 2205 duplex stainless steels in cathode PEMFCs environment. The current densities of two stainless steels decrease rapidly in the beginning, which indicates the formation of protective passive films on the surface of the two stainless steels in cathode PEMFCs environment. Then, the current increases and gradually stabilizes. It can be seen that surface molybdenum-enriched 2205 duplex stainless steel has evident lower steady current density than solid solution one in cathode PEMFCs environment, which is agreed with results from potentiodynamic polarization curves. Mo alloying and homogenization heat treatment were found to have a beneficial effect on the corrosion behavior of ferritic stainless steel in 0.1 M

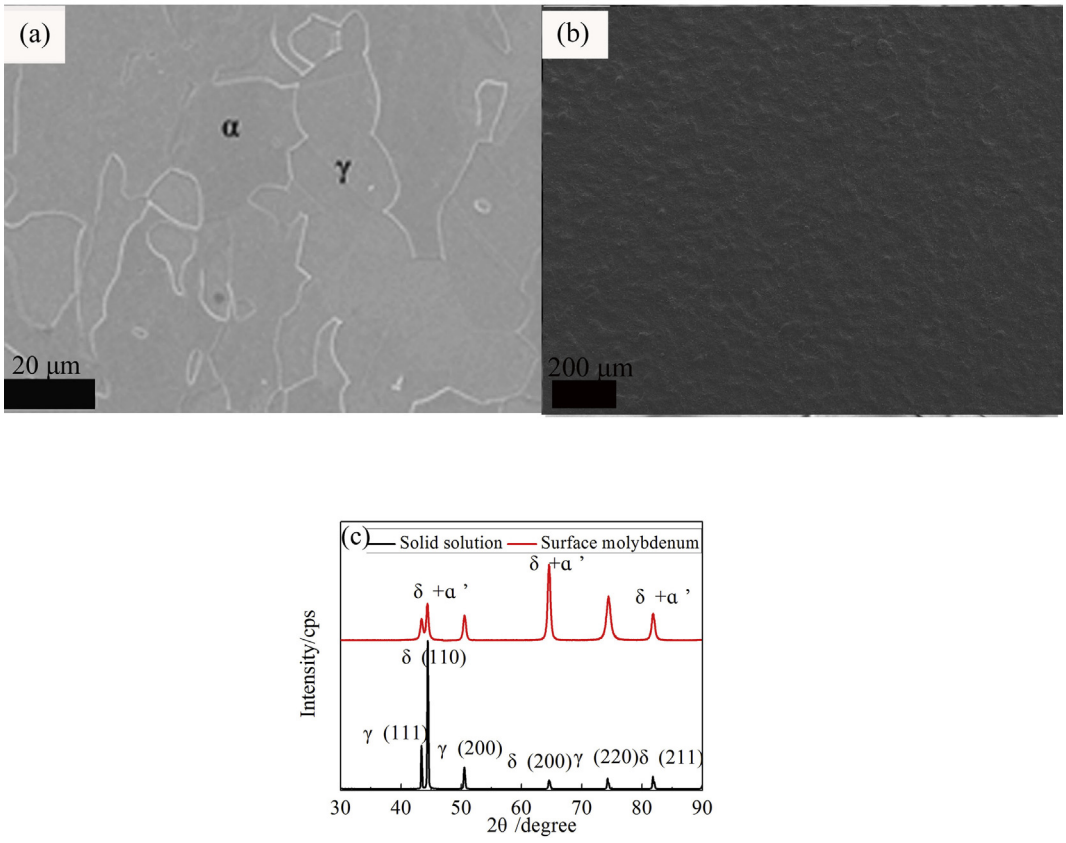

Fig. 1. The microstructures of (a) solid solution and (b) surface molybdenum-enriched 2205 duplex stainless steel, (c) the XRD patterns for solid solution and surface molybdenum-enriched 2205 duplex stainless steels.

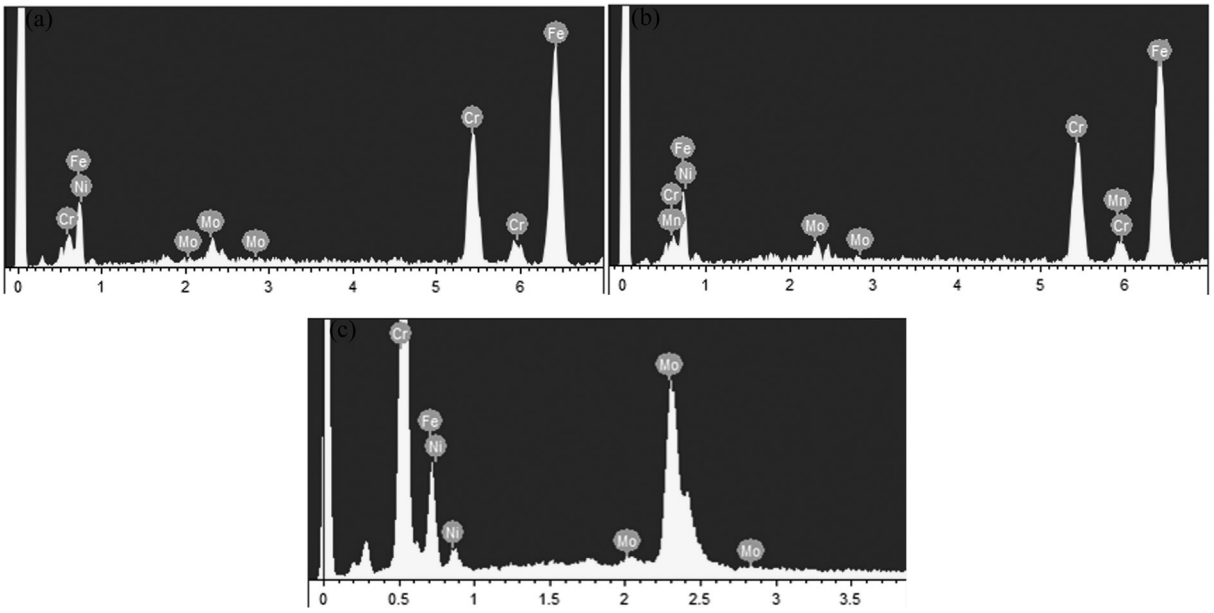

Fig. 2. Chemical compositions of (a) ferritic phase and (b) austenitic phase in solid solution 2205 duplex stainless steel and (c) surface molybdenum-enriched 2205 duplex stainless steel.

H_2SO_4 and 0.3 M HCl acid solutions compared with results obtained from experiments performed on unalloyed one [15].

EIS is also used to determine the stability of the passive films formed on the stainless steels in PEMFCs environment [16]. The impedance spectra were measured at 0.6 V_{SCE} after potentiostatic test. The Nyquist plots of solid solution and surface molybdenum-enriched 2205 duplex stainless steels in cathode PEMFCs environment are shown in Fig. 4a. The semicircle diameter of the Nyquist plots of surface molybdenum-enriched 2205 duplex stainless steel is larger than that of solid solution one in cathode

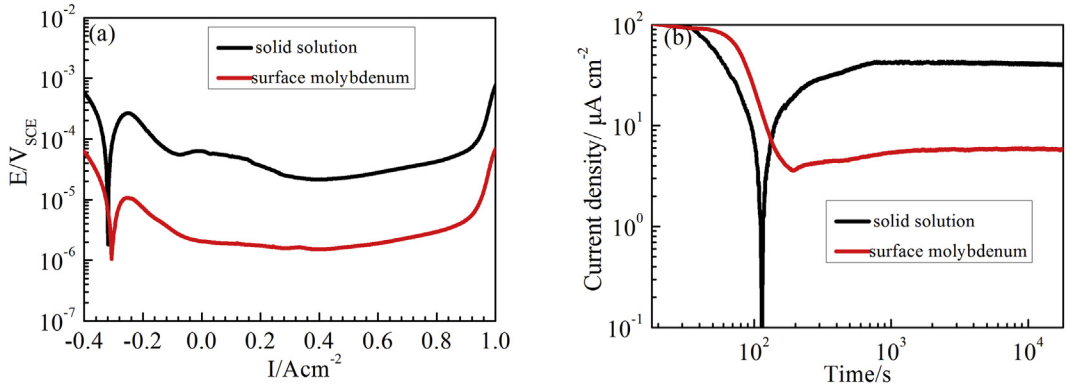

Fig. 3. (a) The potentiodynamic polarization curves and (b) transient currents for solid solution and surface molybdenum-enriched 2205 duplex stainless steels in 0.5 M H_2SO_4 with 2 ppm HF solution at 70 °C bubbled with air.

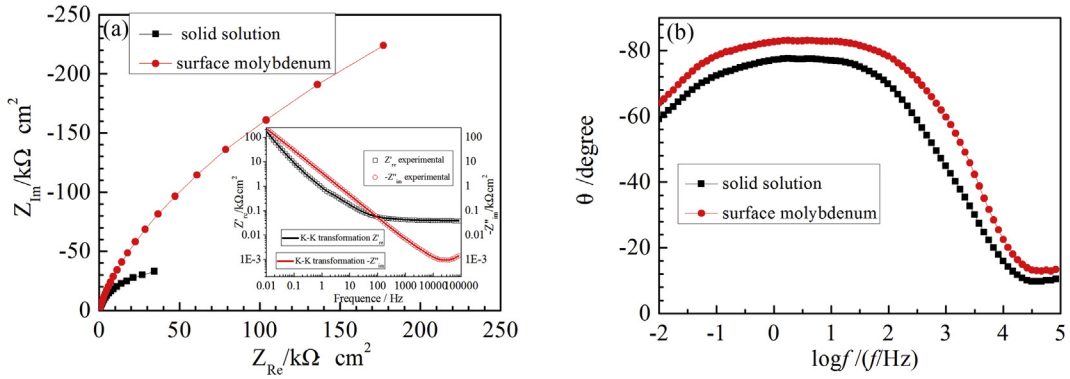

Fig. 4. (a) The Nyquist plots and (b) Bode plots for solid solution and surface molybdenum-enriched 2205 duplex stainless steels in 0.5 M H_2SO_4 with 2 ppm HF solution at 70 °C bubbled with air. Insert showing K–K transformation of the EIS data for surface molybdenum-enriched 2205 duplex stainless steel.

PEMFCs environment. This demonstrates the former has higher corrosion resistance than the latter in cathode PEMFCs environment [17]. The stability of the system of the EIS tests can be effectively evaluated by Kramers–Kronig (K–K) transforms which can be used to validate the data and examine the linearity, causality and stability constraints of the system based on Linear Systems Theory (LST) [18]. The transforming the real axis into the imaginary axis and the imaginary axis into the real axis was applied to the experimental impedance data by K–K transforms and experimental data. A good agreement between the impedance data and corresponding K–K transforms has be observed for surface molybdenum-enriched 2205 duplex stainless steel in inset in Fig. 4a. This indicates that the system satisfies the constraints of LST. One time constant is observed in Bode plots in Fig. 4b. In addition, surface molybdenum-enriched 2205 duplex stainless steel has higher phase angle than solid solution one, which indicates more compact passive film formed on surface molybdenum-enriched 2205 duplex stainless steel in cathode PEMFCs environment. The higher molybdenum content and nitrogen content improved the corrosion resistance of the 2205 duplex stainless steel bipolar plates in cathode PEMFCs environment [19]. The above tests also indicate that surface molybdenum-enriched 2205 duplex stainless steel is more suitable as the bipolar plates in cathode PEMFCs environment due to its excellent corrosion resistance.

The Mott–Schottky measurements were carried out to evaluate the semiconductor characteristic of the passive films. The space charge capacitances of *n*-type and *p*-type semiconductors of the passive films are approximately given by Eqs. (1) and (2), respectively [20]

$$C^{-2} = C_H^{-2} + C_{SC}^{-2} = \frac{2}{\varepsilon_S \varepsilon_0 q N_D}\left(E - E_{fb} - \frac{kT}{e}\right) \quad (1)$$

$$C^{-2} = C_H^{-2} + C_{SC}^{-2} = \frac{-2}{\varepsilon_S \varepsilon_0 q N_A}\left(E - E_{fb} - \frac{kT}{e}\right) \quad (2)$$

where ε_0 is the vacuum permittivity (8.854×10^{-12} Fm^{-1}); ε_s is the relative dielectric constant of the corresponding passive film, which is taken to be 12 for the passive films formed on stainless steels [21]; e is the electron charge (1.6×10^{-19} C); k is the Boltzmann constant (1.38×10^{-23} JK^{-1});N_D and N_A is the donor and acceptor density in passive films, respectively; T is the absolute temperature; E and E_{fb} is applied potential and flatband potential, respectively.

Fig. 5a shows the Mott-Schottky plots of solid solution and surface molybdenum-enriched 2205 duplex stainless steels after applied potentiostatic polarizations in 0.5 M H_2SO_4 with 2 ppm HF solution at 70 °C bubbled with air. Each plot reveals two straight regions with a positive and a negative slopes separated by a narrow potential plateau range. The negative slope under flatband potential demonstrates the behavior of the *p*-type semiconductor characteristic, while the positive slope above flatband potential shows the behavior of a *n*-type semiconductor characteristic. According to point defect model [22], predominant acceptor species are cation vacancies in passive films, while major donor species are oxygen vacancies and/or cation interstitials. The negative and positive slopes in Mott-Schottky plots indicate that the duplex structure of passive film is formed on the surface of 2205 duplex stainless steels [23,24]. The outer layer of the passive film could be enriched in Fe and Mo oxides, while inner layer of the passive film could be enriched in the Cr oxides [25]. The donor and

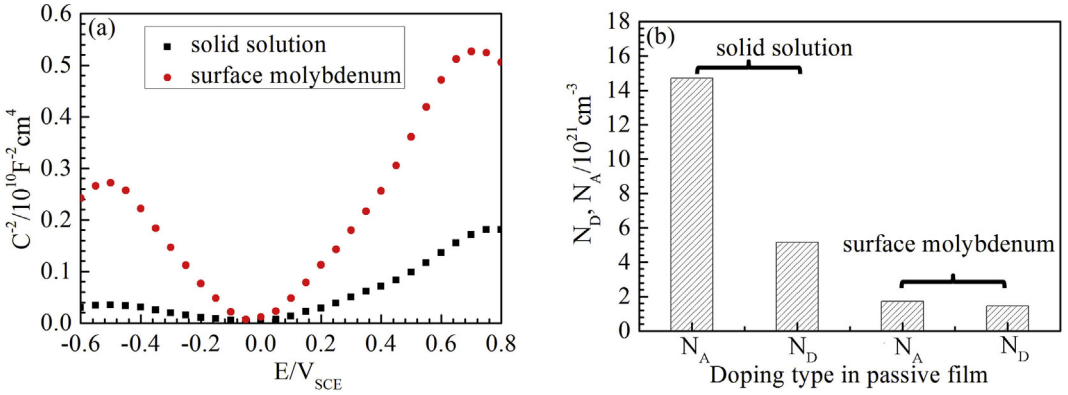

Fig. 5. (a) The Mott-Schottky plots for solid solution and surface molybdenum-enriched 2205 duplex stainless steels in 0.5 M H_2SO_4 with 2 ppm HF solution at 70 °C bubbled with air, (b) the donor and acceptor concentrations in the passive films.

acceptor concentrations in passive films are calculated from the corresponding linear segments in the Mott-Schottky plots, and the corresponding results are shown in Fig. 5b. It is obvious that donor and acceptor concentrations decrease significantly due to surface enriched molybdenum, especially for acceptor density. Therefore, it can be predicted that decreased donor and acceptor concentrations improve corrosion resistance of surface molybdenum-enriched 2205 duplex stainless steel bipolar plates in the simulated cathodic PEMFCs environment [26].

Fig. 6a and b show the Mo XPS spectra of the passive films formed on solid solution and surface molybdenum-enriched 2205 duplex stainless steels in cathode PEMFCs environment. The Mo 3d spectrum consists of three peaks which are designated as metal molybdenum, MoO_3 and MoO_2, respectively [27]. In addition, the Mo-oxide content increases on surface molybdenum-enriched 2205 duplex stainless steel. More molybdenum oxides in passive film could significantly improve the corrosion resistance of surface molybdenum-enriched 2205 duplex stainless steel bipolar plates in cathode PEMFCs environment.

The ICR of the solid solution and surface molybdenum-enriched 2205 duplex stainless steel bipolar plates and the carbon paper is shown in Fig. 7 as a function of compaction force from 50 to 500 N cm^{-2}. The contact resistance reduces with the increasing of the compaction force [28]. This is attributed to an increase in effective contact area [29]. The surface roughness could affect also surface contact resistance. Rough surfaces resulted in small share of contact area, which thus induced a high ICR value [30]. It was found that the corrosion resistance and conductivity of plasma nitrided stainless steel as bipolar plates improved significantly

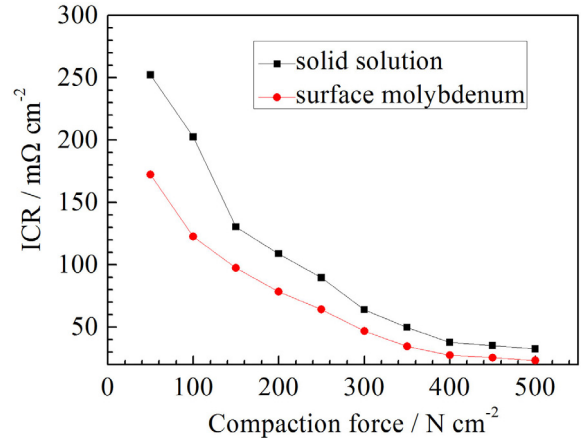

Fig. 7. The ICR of solid solution and surface molybdenum-enriched 2205 duplex stainless steels with carbon paper as a function of compaction force.

due to the rich chromium layer and the low roughness of the modified passive layer [31]. The surface of polypyrrole-camphorsulfonic acid coating on 304 stainless steel bipolar plates with less rough had the lower current density and the lower ICR [32]. However, compared with pure Ni, Fe and Cr, pure Mo shows higher electrical conductivity. In addition, the ball milling induces rough surface which might act as contacts for transportation of electrons. Moreover, surface defect also could facilitate diffusing of the electrolyte. In short, current obtained surface

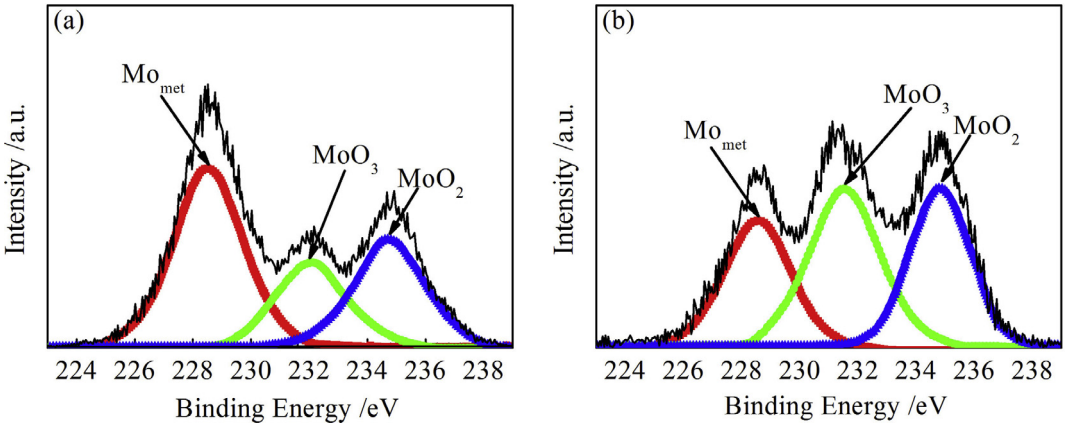

Fig. 6. The detailed XPS spectra of Mo 3d of the passive films formed on (a) solid solution and (b) surface molybdenum-enriched 2205 duplex stainless steels in 0.5 M H_2SO_4 with 2 ppm HF solution at 70 °C bubbled with air.

molybdenum-enriched 2205 duplex stainless steel bipolar plates have lower contact resistance than solid solution one. The low ICR values could lead to low ohmic losses in PEMFCs [33] and could increase the durability of the fuel cell stack. According to results of the corrosion resistance and the ICR, it can be inferred that surface molybdenum-enriched 2205 duplex stainless steel is suitable as metallic bipolar plates for applications in PEMFCs environment.

Conclusions

The effect of surface molybdenum enrichment on the corrosion behaviors and the ICR of the 2205 duplex stainless steel bipolar plates in the simulated cathodic PEMFCs environment was investigated. The main conclusions were as follows:

1) Surface molybdenum-enriched 2205 duplex stainless steel was obtained by ball milling technique.
2) Higher molybdenum content on the surface of 2205 duplex stainless steel bipolar plates improved its corrosion resistance in cathode PEMFCs environment.
3) The surface molybdenum enrichment on 2205 duplex stainless steel bipolar plates decreased donor and acceptor concentration in passive films and improved significantly its corrosion resistance in cathode PEMFCs environment.
4) The ICR value of the 2205 duplex stainless steel bipolar plates decreased after surface molybdenum enrichment by ball milling.

Acknowledgements

This work was financially supported by National Natural Science Foundation of China (Grant No. 91326203).

Appendix A. Supplementary data

Supplementary data associated with this article can be found, in the online version, at http://dx.doi.org/10.1016/j.rinp.2017.09.001.

References

[1] Steele BCH, Heinzel A. Materials for fuel-cell technologies. Nature 2001;414:345–6.
[2] Taherian R. A review of composite and metallic bipolar plates in proton exchange membrane fuel cell: Materials, fabrication, and material selection. J Power Sources 2014;265:370–90.
[3] Wang H, Sweikart MA, Turner JA. Stainless steel as bipolar plate material for polymer electrolyte membrane fuel cells. J Power Sources 2003;115:243–51.
[4] Kelly MJ, Fafilek G, Besenhard JO, Kronberger H, Nauer GE. Contaminant absorption and conductivity in polymer electrolyte membranes. J Power Sources 2005;145:249–52.
[5] Dutta Majumdar J, Manna I. Laser surface alloying of AISI 304-stainless steel with molybdenum for improvement in pitting and erosion-corrosion resistance. Mater Sci Eng, A 1999;267:50–9.
[6] Pardo A, Merino MC, Coy AE, Viejo F, Arrabal R, Matykina E. Effect of Mo and Mn additions on the corrosion behaviour of AISI 304 and 316 stainless steels in H_2SO_4. Corros Sci 2008;50:780–94.
[7] Montemor MF, Simões AMP, Ferreira MGS, Belo MDC. The role of Mo in the chemical composition and semiconductive behaviour of oxide films formed on stainless steels. Corros Sci 1999;41:17–34.
[8] Vignal V, Olive JM, Desjardins D. Effect of molybdenum on passivity of stainless steels in chloride media using ex situ near field microscopy observations. Corros Sci 1999;41:869–84.
[9] Hashimoto K, Asami K, Teramoto K. An X-ray photo-electron spectroscopic study on the role of molybdenum in increasing the corrosion resistance of ferritic stainless steels in HC1. Corros Sci 1979;19:3–14.
[10] Wang LX, Sun JC, Li PB, Sun J, Lv Y, Jing B, Li S, Ji SJ, Wen ZS. Molybdenum nitride modified AISI 304 stainless steel bipolar plate for proton exchange membrane fuel cell. Int J Hydrogen Energy 2012;37:5876–83.
[11] Li DG, Wang JD, Chen DR, Liang P. Molybdenum addition enhancing the corrosion behaviors of 316 L stainless steel in the simulated cathodic environment of proton exchange membrane fuel cell. Int J Hydrogen Energy 2015;40:5947–57.
[12] Zhang M, Kim KH, Shao ZG, Wang FF, Zhao S, Suo N. Effects of Mo content on microstructure and corrosion resistance of arc ion plated Ti-Mo-N films on 316L stainless steel as bipolar plates for polymer exchange membrane fuel cells. J Power Sources 2014;253:201–4.
[13] Kim YS. Influences of alloyed molybdenum and molybdate addition on the corrosion properties and passive film composition of stainless steels. Met Mater Int 1998;4:183–91.
[14] Liu G, Lu J, Lu K. Surface nanocrystallization of 316L stainless steel induced by ultrasonic shot peening. Mater Sci Eng A 2000;286:91–5.
[15] Demiroren H, Aksoy M, Yildiz T, Buytoz S. The corrosion characterization of a ferritic stainless steel with Mo addition in H_2SO_4 and HCI acid solutions. Prot Met Phys Chem+ 2009;45:628–34.
[16] Wang LX, Sun JC, Kang B, Li S, Ji SJ, Wen ZS, Wang XC. Electrochemical behaviour and surface conductivity of niobium carbide-modified austenitic stainless steel bipolar plate. J Power Sources 2014;246:775–82.
[17] Udhayan R, Bhatt DP. On the corrosion behaviour of magnesium and its alloys using electrochemical techniques. J Power Sources 1996;63:103–7.
[18] Nicic I, Macdonald DD. The passivity of Type 316L stainless steel in borate buffer solution. J Nucl Mater 2008;379:54–8.
[19] Lin KJ, Li XY, Sun Y, Luo X, Dong HS. Active screen plasma nitriding of 316 stainless steel for the application of bipolar plates in proton exchange membrane fuel cells. Int J Hydrogen Energy 2014;39:21470–9.
[20] Williamson J, Isgor OB. The effect of simulated concrete pore solution composition and chlorides on the electronic properties of passive films on carbon steel rebar. Corros Sci 2016;106:82–95.
[21] Dean MH, Newmark AR, Stimming U. On the evaluation of the flatband potential from photocurrent measurements. J Electroanal Chem 1988;244:307–10.
[22] Macdonald DD. The history of the Point Defect Model for the passive state: a brief review of film growth aspects. Electrochim Acta 2011;56:1761–72.
[23] Lv JL, Liang TX, Wang C, Dong LM. Comparison of corrosion properties of passive films formed on coarse grained and ultrafine grained AISI 2205 duplex stainless steels. J Electroanal Chem 2015;757:263–9.
[24] Oguzie EE, Li JB, Liu YQ, Chen DM, Li Y, Yang K, Wang FH. The effect of Cu addition on the electrochemical corrosion and passivation behavior of stainless steels. Electrochim Acta 2010;55:5028–35.
[25] Luo H, Su HZ, Dong CF, Li XG. Passivation and electrochemical behavior of 316L stainless steel in chlorinated simulated concrete pore solution. Appl Surf Sci 2017;400:38–48.
[26] Lv JL, Luo HY, Liang TX, Guo WL. The effects of grain refinement and deformation on corrosion resistance of passive film formed on the surface of 304 stainless steels. Mater Res Bull 2015;70:896–907.
[27] Xu J, Zhou CG, Jiang SY. Investigation on corrosion behavior of sputter-deposited nanocrystalline (Mo x Cr 1− x) 5Si3 films by double cathode glow plasma. Intermetallics 2010;18:1669–75.
[28] Bi FF, Yi PY, Zhou T, Peng LF, Lai XM. Effects of Al incorporation on the interfacial conductivity and corrosion resistance of CrN film on SS316L as bipolar plates for proton exchange membrane fuel cells. Int J Hydrogen Energy 2015;40:9790–802.
[29] Xu J, Li ZY, Xu S, Munroe P, Xie ZH. A nanocrystalline zirconium carbide coating as a functional corrosion-resistant barrier for polymer electrolyte membrane fuel cell application. J Power Sources 2015;297:359–69.
[30] Wlodarczyk R, Zasada D, Morel S, Kacprzak A. A comparison of nickel coated and uncoated sintered stainless steel used as bipolar plates in low-temperature fuel cells. Int J Hydrogen Energy 2016;41:17644–51.
[31] Dadfar M, Salehi M, Golozar MA, Trasatti S. Surface modification of 304 stainless steels to improve corrosion behavior and interfacial contact resistance of bipolar plates. Int J Hydrogen Energy 2016;41:21375–84.
[32] Jiang L, Syed JA, Gao YZ, Zhang QX, Zhao JF, Lu HB, Meng XK. Electropolymerization of camphorsulfonic acid doped conductive polypyrrole anti-corrosive coating for 304SS bipolar plates. Appl Surf Sci 2017;426:87–98.
[33] Jin CK, Lee KH, Kang CG. Performance and characteristics of titanium nitride, chromium nitride, multi-coated stainless steel 304 bipolar plates fabricated through a rubber forming process. Int J Hydrogen Energy 2015;40:6681–8.